

ADVANCEMENTS OF THE MANUFACTURING TECHNOLOGY WITH HIGH-PRESSURE LIQUID CO₂ JETS

E. Uhlmann, P. John
Technische Universität Berlin
Berlin, Germany

ABSTRACT

The main advantages of cutting with liquid jets are the flexibility and consistently sharp tool, which allows the machining of a large number of materials and complex shapes. Unfortunately, the humidification of the components is a problem for certain applications and inhibits the spread of jet technology. In contrast, jetting with liquid carbon dioxide (CO₂) offers new potentials in the field of dry and residue-free cutting processes. In the recent past, a prototypical system was developed which allowed the generation of a stable liquid CO₂ jet and its analyzation. Due to that, producible jet forces, jet velocities and cut notches depending on machining parameters like nozzle diameter, jet pressure and jet distance were investigated.

With this publication the jet modification and optimization in order to achieve a competitive industrial manufacturing process will be presented. In the investigation on the jetting with high-pressure CO₂ with up to 300 MPa the jet performance on different materials will be analyzed and compared with the plain waterjet machining. Therefore especially the impact of the working distance will be investigated.

1 INTRODUCTION

Water jet machining has developed to a multifunctional tool for processing various technical materials. The main advantages of the technology, like continuous transport of chips, high flexibility and the availability of a persistent sharp tool with low thermal and mechanical load on the workpieces, still open up new fields of applications. For some applications, water jetting will never be the first choice of machining technology due to its additional process steps such as the microfiltration before as well as the post-treatment with disposal of water, cleaning and drying of the workpieces after machining [1, 2]. The non-sterile process and humidification, unhelpful for example in medical or cleanroom applications, are limiting factors of conventional jet processes and motivate to search for alternative cutting methods.

Due to the complete sublimation of the jet medium, jet cutting with carbon dioxide (CO₂) is a dry and residue-free process. The used CO₂ is a waste product of industrial processes and can be considered as environmentally neutral [3]. Snow blasting with solid CO₂ was established in recent years for pretreating and decoating [4] but the low hardness of the particles prevents the ability to be more than a cleaning process. Therefore jetting with liquid CO₂ represents an alternative option.

High-pressure jet cutting with liquid CO₂ as a jet medium was first investigated in a feasibility study by DUNSKY and HASHISH [5]. They proved the realizability of the process under atmospheric conditions and showed similarities to water jet cutting as a residue-free cutting process. Based on these results BILZ [6] designed a prototype system at the Production Technology Centre Berlin (PTC) and continued with detailed analytical and experimental investigations. Force impulse measurements and the evaluation of kerf characteristics on plastic specimens were conducted to show the industrial potential of the high-pressure jet cutting process. Originating from a joint research project with the PTC, ENGELMEIER [7] carried on investigations in order to analyze pressures and temperatures in the process and their influence on jet deformation and decay.

In previous work [8] a general suitability of the process for a dry and residue-free cutting of metal materials was proved. Investigations on jet velocity, jet impulse force and kerf geometry on aluminum specimen (AlMg₃) using jet pressures up to 300 MPa led to knowledge about main differences between plain water jet cutting and jetting with liquid CO₂.

Continuing, in this paper the depth of cut for certain materials depending on various influencing factors will be shown. Not only for obvious process parameters like pressure and nozzle diameter, but also the working distance will be examined. Furthermore, the secondary material damage will be investigated.

2 TEST STAND AND MEASUREMENT SETUP

2.1 Test stand for liquid CO₂ jets

By using a prototype system functional correlations between significant setting parameters and results were developed analytically and experimentally in order to analyze the cutting properties of the CO₂ jet. The significant factors are the depth of cut k_T and the middle kerf width k_{BM} .

Following, the test stand and the measuring principle to analyze these quantities are described. The empirical investigations on the plain water jet cutting technology were performed with the system Jet Max HRX 160L from MAXIMATOR JET GMBH, Schweinfurt, Germany, with a high-pressure pump HPS 6045 which realizes jet pressures up to $p_0 = 600$ MPa.

The liquid CO₂ cutting jet system is divided into three functional modules: Climatic chamber, high-pressure pump and cutting chamber (Figure 1). The liquid CO₂ is supplied from a riser pipe bottle inside the chamber via high-pressure hoses to the suction side of the high-pressure pump. According to the temperature inside the climatic chamber, the supply pressure is regulated up to $p_v = 9$ MPa at 45 to 50 °C. Within the pump, liquid carbon dioxide is gradually compressed up to 300 MPa and pumped to the pulsation damper to the closed cutting head in the cutting chamber. The high-pressure pump is a Steamline1 of INGERSOLL-RAND, Swords, Ireland, with a maximum pressure of $p_0 = 345$ MPa and a maximum flow rate of $Q = 3.8$ l/min. The cutting head is pneumatically actuated and opened, allowing the high-pressure fluid to exit the nozzle. The cutting head, Active Autoline II from KMT GMBH, Bad Nauheim, Germany, attached to the gantry robot is moved according to the chosen direction and at the selected feed speed. The machining of the part with the high-pressure CO₂ jet takes place on a worktable where the workpieces are fixed. The removed material falls through a grating and can be collected and analysed afterwards.

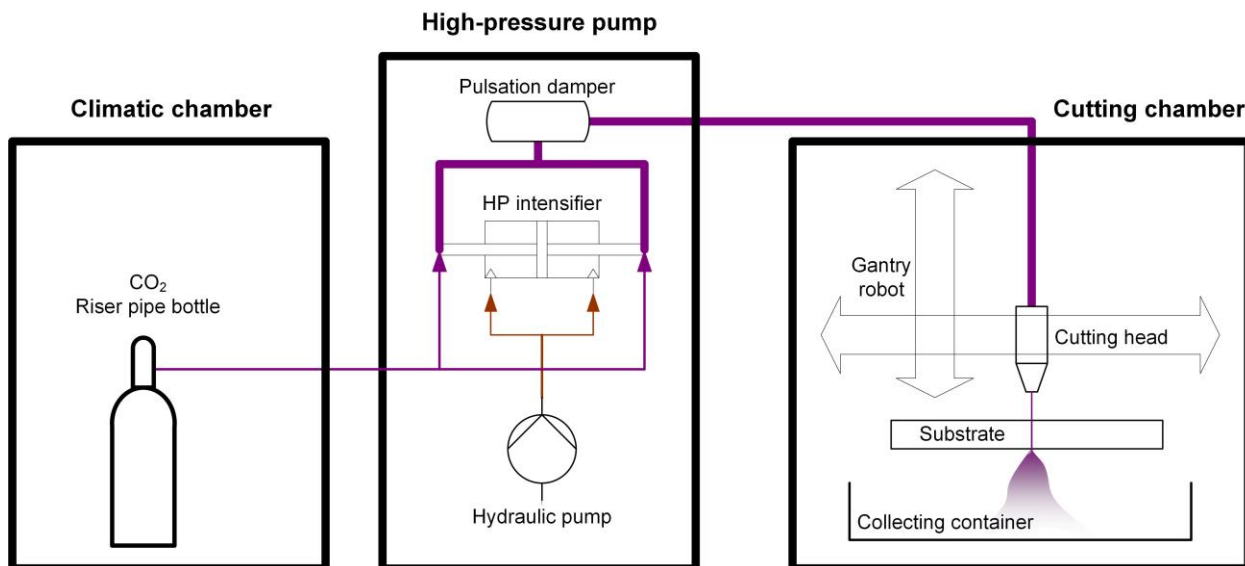


Figure 1. Schematic sketch of the high-pressure liquid CO₂ jet cutting system

2.2 Measurement of kerf characteristics

To analyze the potential of creating kerfs, the depth of cut k_T , kerf width k_B , middle kerf width k_{BM} and kerf shape k_F were investigated. The middle kerf width was measured at half of the depth of cut. The kerf shape k_F is a qualitative value and compares the kerf profile along the abscissa axis by cutting vertically through the kerf (Figure 2). For these investigations the specimen of rolled sheet with a thickness of 2 mm consisting of the aluminum alloy AlMg₃ were processed with different parameters. The material was chosen due to the characteristic properties of metal, but low hardness. Previous results of the jet impulse forces F_s [8] as well as preliminary tests led to the

that the depth of cut k_T has similar values for the nozzle diameters $d_D = 0.20$ mm and $d_D = 0.25$ mm. The smaller nozzle even achieves higher depths of cut in some cases. That contradicts the other results and could be related to a further limiting factor of the system - the limited volume flow rate caused by the riser pipe bottle. In future work this has to be excluded.

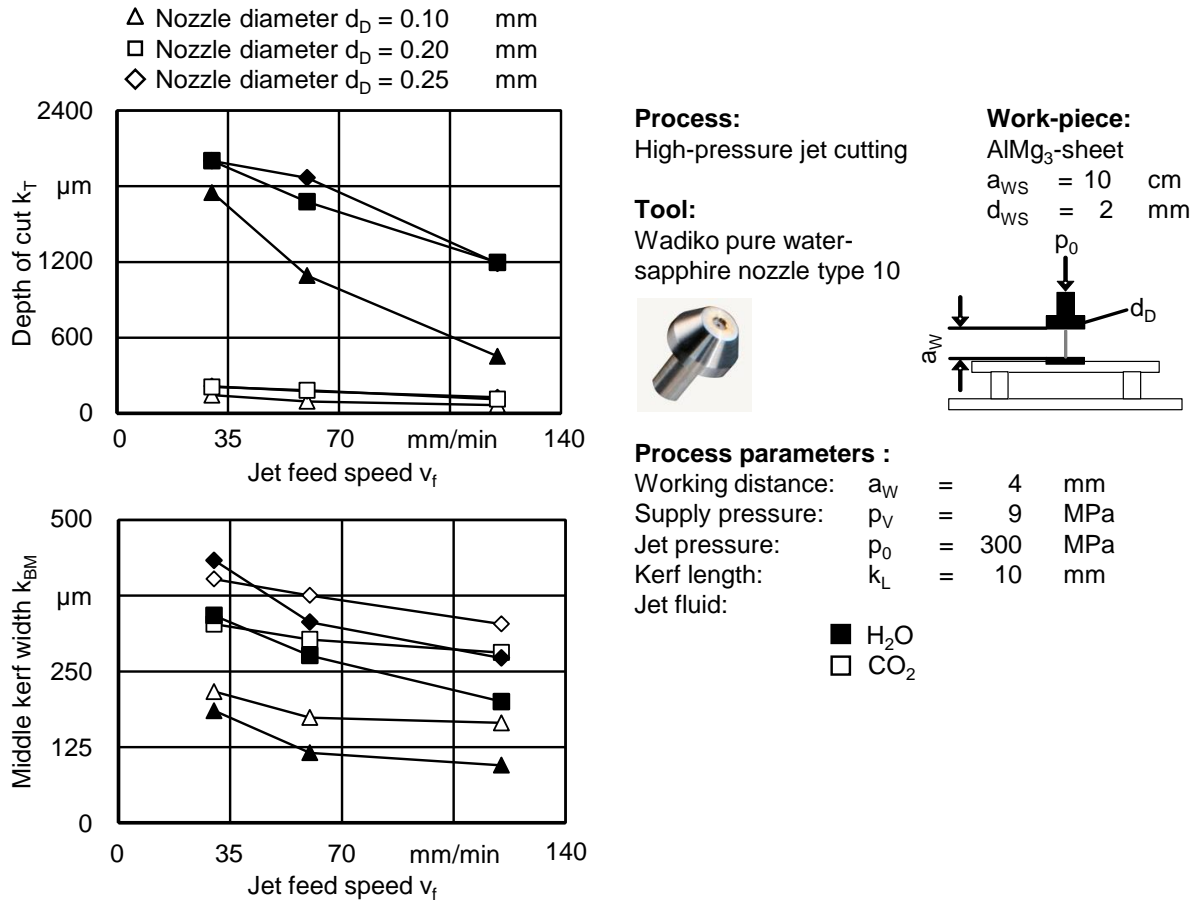


Figure 3. Depth of cut k_T und middle kerf width K_{BM} depending on jet feed speed v_f

The investigation of the cutting surface in lateral view showed a characteristic outcome for the plain waterjet (Figure 4b). The images, taken with the Dino-Lite edge digital microscope from ANMO ELECTRONICS CORPORATION, Taiwan, show that the surface is divided into three zones: The clear cutting lines near the workpiece surface; the pretty clear transition zone; the rough cutting surface with drag line separation due to the feed speed. Quite different is the cutting result after jetting with liquid CO₂. The cutting surface shows a rather pore-like characteristic and the kerf root is wavy and rough. These results indicate a significant difference at the behavior of the backwater between liquid CO₂ and water. The density difference and gaseous phase seem to manifest here.

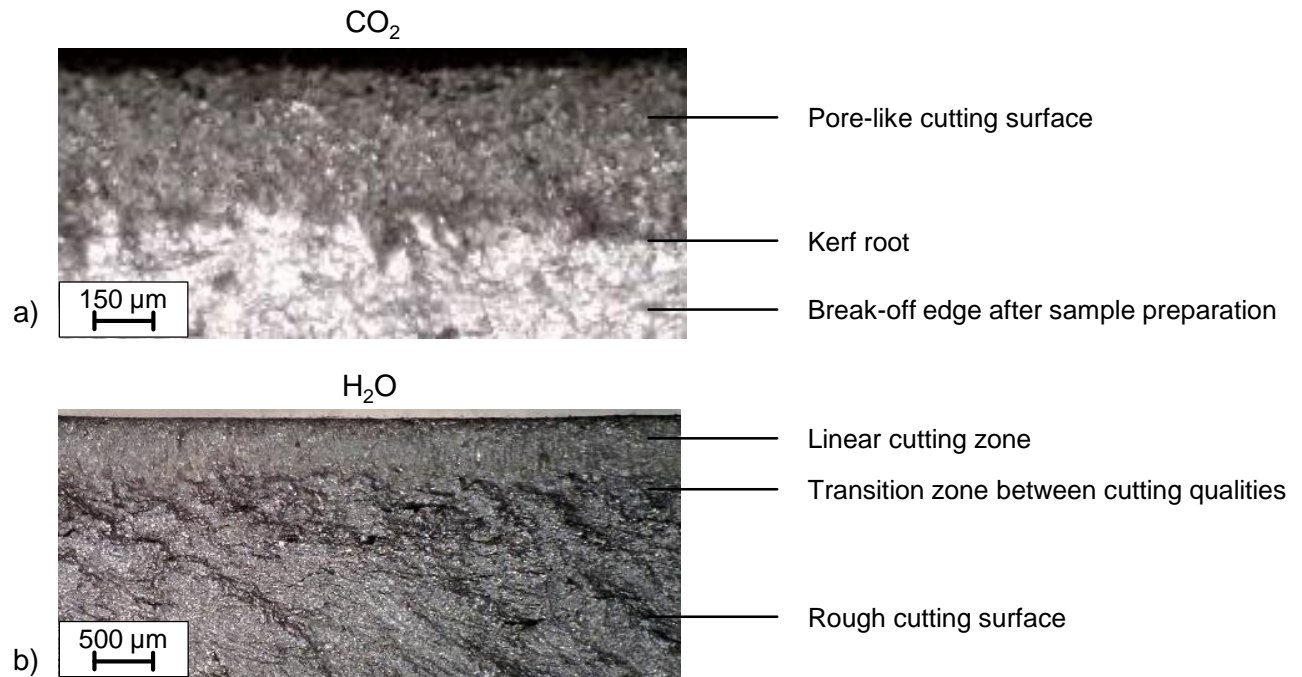
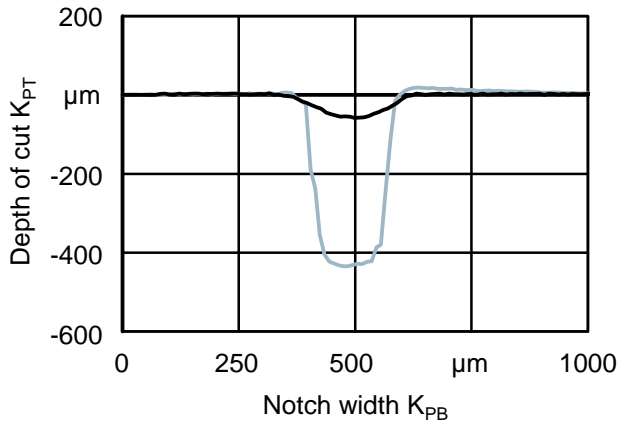


Figure 4. Lateral cutting surface for $p_0 = 300$ MPa, $v_f = 30$ mm/min, $a_w = 4$ mm; a) CO₂ jet, $d_D = 0.12$ mm; b) H₂O jets, $d_D = 0.25$ mm

The evaluation of the kerf geometries in cross direction resulted in a V-shaped kerf profile for all feed speeds v_f for the jet fluid CO₂. By using plain water the depth k_T significantly increased and a rather U-shaped kerf profile was identified. That indicates a multiphase state of the CO₂ jet, which means that the density and therefore the cutting performance are higher inside the jet (Figure 5).



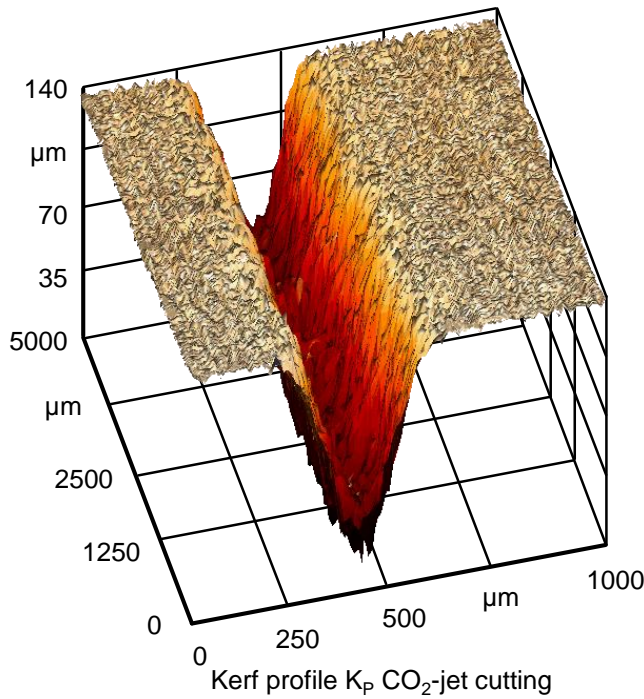
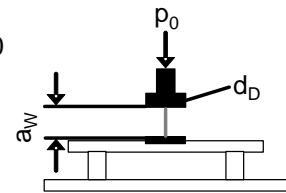
Process:
High-pressure jet cutting

Tool:
Wadiko pure water-sapphire nozzle type 10



Work-piece :

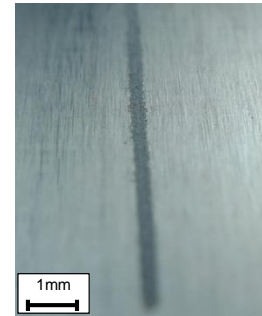
AlMg₃-sheet
a_{WS} = 10 cm
d_{WS} = 2 mm



Process parameters :

Nozzle diameter: $d_D = 0.1$ mm
Working distance: $a_W = 4.0$ mm
Jet feed speed: $v_f = 60.0$ mm/min
Supply pressure: $p_V = 9.0$ MPa
Jet pressure: $p_0 = 300.0$ MPa
Kerf length: $k_L = 10.0$ mm
Jet fluid:

■ CO₂
■ H₂O



CO₂-jet cutting of AlMg₃

Figure 5. Comparison of kerf geometries with CO₂ and H₂O as jet fluids

This assumption is illustrated in [Figure 6](#). It can be seen, that the jet is fraying at the edge and wave formation occurs. Only at increasing jet pressure the inside of the jet can be identified as homogeneous liquid CO₂, shown in [Figure 6b](#). By increasing the jet pressure from $p_0 = 100$ MPa to $p_0 = 300$ MPa the jet characteristics regarding cutting performance, homogeneity and jet expansion directly after the nozzle outlet could be influenced positively. As shown in [Figure 6](#), the jet expands after the nozzle outlet and widens with increasing distance. The jet diameter after the nozzle outlet is $d_{S1} = 1.08$ mm for the nozzle diameter $d_D = 0.1$ mm. This equates to an expansion by a factor of 10. The cutting performance at the workpiece only achieved a middle kerf width of $k_{BM} < 0.2$ mm, which corresponds approximately to the homogeneous liquid jet center. The expansion of the CO₂ is caused by the extreme pressure drop at atmospheric conditions and a concurrent temperature change directly after the nozzle outlet. Thus, the jet fluid CO₂ changes from liquid state to gaseous state at the outer edge of the jet.

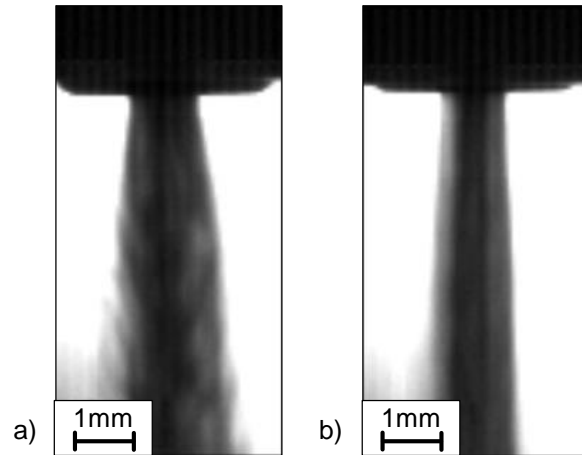
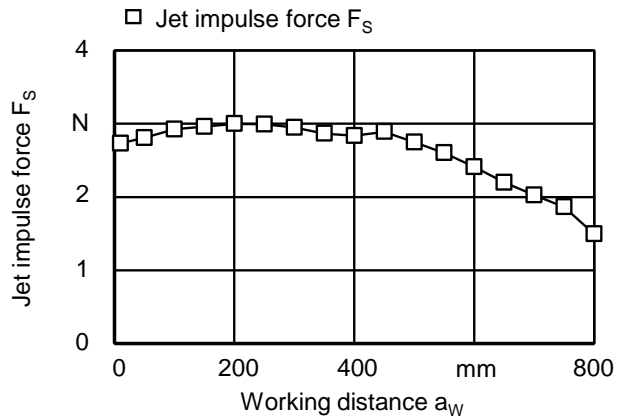


Figure 6. CO₂ jet with $d_D = 0.1$ mm at; a) $p_0 = 100$ MPa; b) $p_0 = 300$ MPa [8]

3.2 The Depth of cut indicates the jet decay

With the measurement setup, detailed described in [8], it is possible to compare the jet impulse force F_S of the fluid with its effect at the workpiece surface. As shown in [Figure 6](#) the jet impulse force F_S decreases not before a working distance of $a_w = 400$ mm in contrast to its effect on the depth of cut k_T which ends at about $a_w = 30$ mm. The kerf width k_B increases for all tested nozzle diameters until a working distance of $a_w = 20$ mm and then drops slightly until no depth of cut was measured. Obviously, the nozzle with a diameter of $d_D = 0.15$ mm achieved the widest kerfs with a maximum of $k_B = 1182$ μm at a working distance of $a_w = 20$ mm. This parameter combination of nozzle diameter, mass flow and jet pressure seems to realize a very stable jet which can be used for machining with the present machine system.

Alongside the jet from nozzle to workpiece, two different characteristics are influencing the decreasing of cutting depth: On one hand, the phase transformation from liquid to gas which inherits a density decrease of the fluid. On the other hand the conical expansion of the jet which enlarges the jet cross-sectional area and therefore decreases the effective area force. A distinct difference between water and liquid CO₂ jetting, enabling the new technology for complex shapes and 3D -operations without jet catcher, for example necessary for machining with industrial robots.

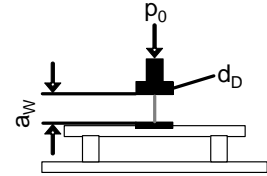


Process:
High-pressure jet cutting

Tool:
Wadiko pure water-sapphire nozzle type 10



Work-piece :
AlMg₃-sheet
 $a_{WS} = 10$ cm
 $d_{WS} = 2$ mm



Process parameters :

Nozzle diameter: $d_D = 0.1$ mm
 Working distance: $a_W = 4.0$ mm
 Jet feed speed: $v_f = 30.0$ mm/min
 Supply pressure: $p_V = 9.0$ MPa
 Jet pressure: $p_0 = 300.0$ MPa
 Kerf length: $k_L = 10.0$ mm
 Jet fluid: CO₂

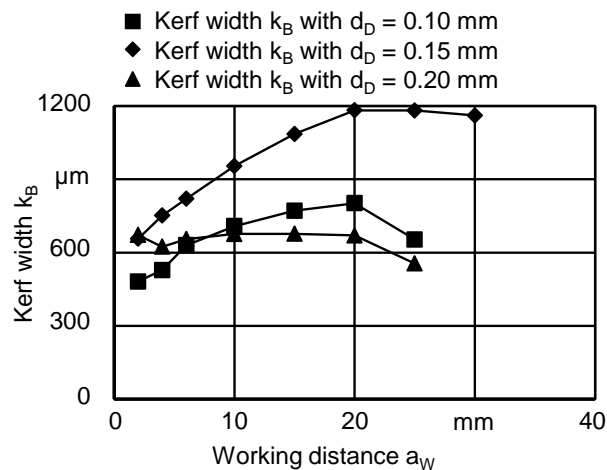
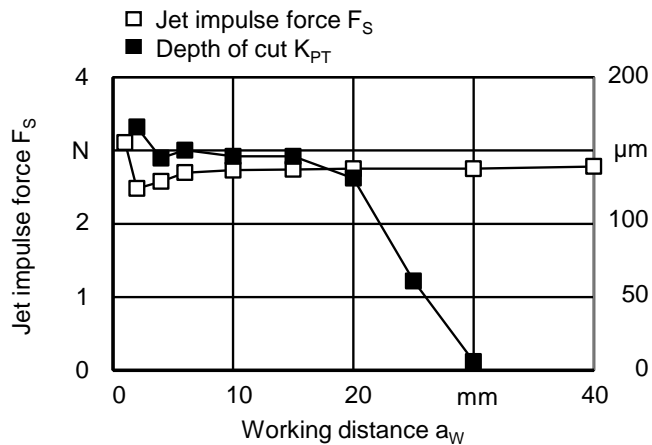


Figure 6. Depth of cut k_T and jet impulse force F_S depending on working distance a_w

In this context it is also interesting how the jet behavior is affected after the penetration of the workpiece. Unfortunately, the CO₂ jet pressure was not effective enough to cut through the AlMg₃ parts, so thin sheets of carbon-fiber reinforced plastic (CFRP) with a material thickness of $d_{WS} = 0.17$ mm were chosen for these investigations. In preliminary tests it was possible to cut CFRP materials with the parameters chosen for AlMg₃ [9]. The investigated CFRP samples were cut through until a maximum working distance $a_{WM} = 25$ mm for the nozzle with $d_D = 0.1$ or $a_{WM} = 40$ mm with $d_D = 0.2$ mm and a jet feed speed of $v_f = 30$ mm/min. To measure the impact

on the secondary workpiece a new experimental setup was realized, as shown in Figure 7. Two sheets were positioned with an angle of $\alpha = 45^\circ$ while jetting with a defined working distance of $a_W = 4$ mm from the first sheet. Through calculation with the trigonometric function (3-1) it is possible to get the secondary working distance a_{SW} at the point k_{L2} , at which still is a depth of cut k_T measurable.

$$\sin(\alpha) = \text{opposite of } \alpha / \text{hypotenuse} \quad (3-1)$$

$$\text{opposite of } \alpha = \sin(\alpha) * \text{hypotenuse} \quad (3-2)$$

$$a_{SW} = \sin(45^\circ) * \text{Kerf length } k_{L2} \quad (3-3)$$

In the course of investigations a differential impact at the workpiece surface has been observed. Due to the structure of the CFRP, with different layers of synthetic resin and filaments, at a certain distance a_{SW} and jet feed speed v_f there was no clear kerf visible but still a damage at the surface was observed. For industrial applications, for example drilling of hollow-chamber profiles, a small damage at the bottom would be criteria for exclusion. The lower feed speed with $v_{f1} = 30$ mm/min and the bigger nozzle led, as expected, to higher working distances with $a_{SW} = 8.4$ mm or rather $a_{SW} = 30$ mm for the two illustrated nozzles. Adding $d_{WS} = 1.7$ mm and $a_W = 4$ mm it is significant, that the CO₂ jet length is shortened and way beyond the original a_{WM} . Consequently, the liquid CO₂ jet not only shows potential for industrial robotic applications, but also for hollow-chamber applications.

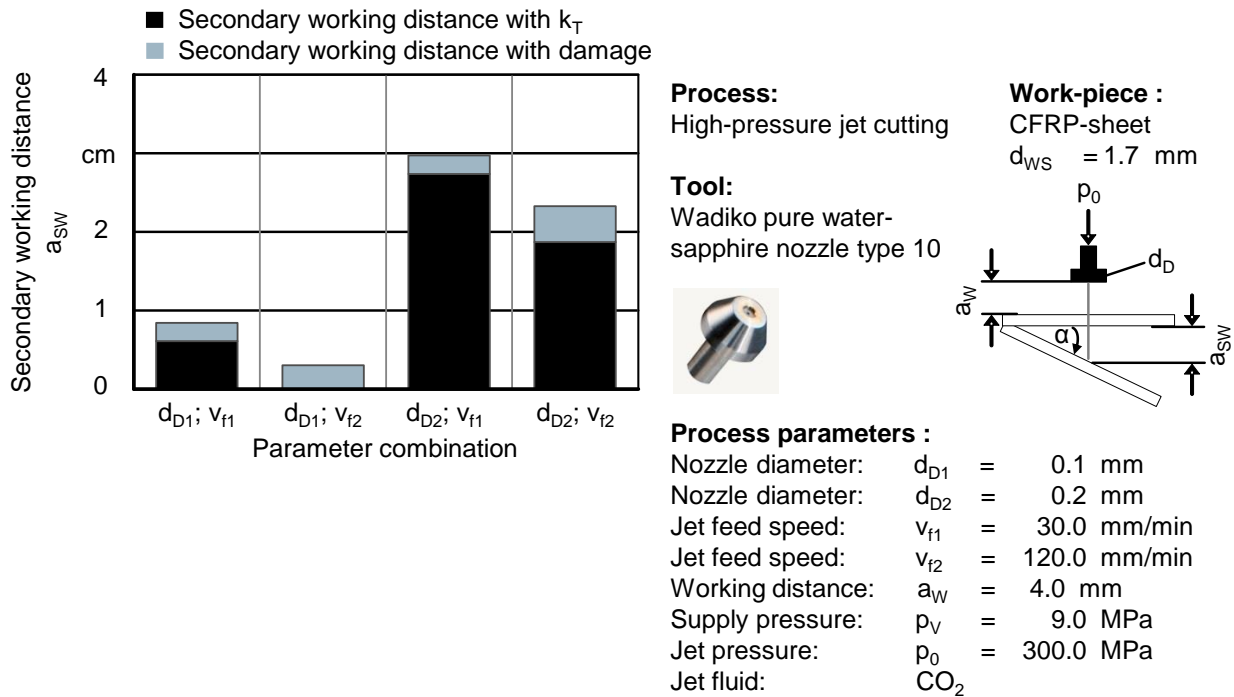


Figure 7. Secondary working distance a_{SW} with a depth of cut k_T and damage of the workpiece

4 CONCLUSIONS

The described experimental and measurement setup provides a coherent and liquid high-pressure

jet of carbon dioxide which is comprehensible and reproducible. The liquid CO₂ jet shows similar behavior to the plain water jet but with slightly lower velocity, force impulse and notch rate. The experiments with specimens of AlMg₃ have shown a general suitability of the process for a dry and residue-free cutting of metal materials. By raising the nozzle diameter d_D and the jet pressure p_0 it was possible to increase the jet impulse force F_s , the jet velocity v_s and the notch effect significantly for both fluids. The raising of the distance between the jet nozzle and the workpieces had no specific influence on jet impulse force F_s in contrast to the kerf geometry. The Kerf depth decreases while the kerf width increases until a certain point, depending on nozzle diameter. The effective liquid CO₂ jet length is especially depending on jet pressure and nozzle diameter and therefore qualified for robotic and hollow-chamber applications. The kerfs after jetting with liquid CO₂ show lateral pore-like cutting sides and v-shapes in cross direction.

Further optimization of the high-pressure CO₂ jet prototype system, like the defined cooling of supply pipes and fluid, as well as a higher mass flow could lead to better results. In further investigations additional parameters will be investigated and other aluminum alloys, plastics and CFRP will be processed to evaluate removal mechanisms.

5 ACKNOWLEDGMENTS

This paper is based on results acquired in the project DFG UH 100/163-3, which is kindly supported by the German Research Foundation (DFG).

6 REFERENCES

- [1] Momber, W. A.; Schulz, R.-R.: Handbuch der Oberflächenbearbeitung Beton – Bearbeitung-Eigenschaften-Prüfung. Basel, Birkhäuser, 2006.
- [2] Kolb, M.: Wasserstrahlschneiden – Materialbearbeitung mit einem Hochdruckwasserstrahl. In: Bibliothek der Technik Band 295. München, Moderne Industrie, 2006.
- [3] Krieg, M. C.: Analyse der Effekte beim Trockeneisstrahlen. Berichte aus dem Produktionstechnischen Zentrum Berlin, Hrsg.: Uhlmann, E. Berlin, Fraunhofer IRB, 2008.
- [4] Uhlmann, E. (Hrsg.); Bilz, M.: Marktstudie Kohlendioxidstrahlen 2010. Fraunhofer-Institut für Produktionsanlagen und Konstruktionstechnik, Berlin, 2010.
- [5] Dunsky, C.; Hashish, M.: Cutting with high pressure CO₂ jets. Allen, A. G. (Hrsg.). Washington: QUEST Integrated, 1994.
- [6] Bilz, M.: Möglichkeiten und Grenzen des Strahlspanens mittels CO₂-Hochdruckstrahlen. Berichte aus dem Produktionstechnischen Zentrum Berlin. Hrsg.: Uhlmann, E. Dissertation, Technische Universität Berlin. Stuttgart: Fraunhofer IRB, 2014.
- [7] Engelmeier, L.: Flüssige, kohärente Kohlendioxidstrahlen zum Schneiden von Materialien in atmosphärischer Umgebung. Berichte aus der Verfahrenstechnik. Dissertation, Ruhr-Universität Bochum. Herzogenrath: Shaker, 2017.
- [8] Uhlmann, E.; John, P.: High-pressure jet cutting with liquid CO₂. In: Proceedings of the 23rd international conference on Water Jetting in Seattle, USA. Hrsg.: BHR Group, 2016, S. 315 - 326.
- [9] Uhlmann, E.; Sammler, F.; Richarz, S.; Heitmüller, F.; Bilz, M.: Machining of Carbon Fibre Reinforced Plastics. Procedia CIRP, Volume 24, 2014, S. 19 - 24.

7 NOMENCLATURE

a_w	Working distance
a_{sw}	Secondary working distance
a_{wm}	Maximum working distance
a_{ws}	Workpiece edge length
d_D	Nozzle diameter
d_{ws}	Workpiece thickness
k_{BM}	Middle kerf width
k_L	Kerf length
k_{L2}	Kerf length at second workpiece
k_T	Depth of cut
p_0	Jet pressure
p_v	Supply pressure
t_s	Jetting time
v_f	Jet feed speed